TRANSVERSE VIBRATIONS OF A ROLLER CHAIN DRIVE WITH TENSIONER

W. Choi and G. E. Johnson
Design Laboratory
Mechanical Engineering and Applied Mechanics
The University of Michigan
Ann Arbor, MI 48109-2125

eagm

UMR1129

TRANSVERSE VIBRATIONS OF A ROLLER CHAIN DRIVE WITH TENSIONER

W. Choi and G. E. Johnson
Design Laboratory
Mechanical Engineering and Applied Mechanics
The University of Michigan
Ann Arbor, MI 48109-2125
Glen_E._Johnson@um.cc.umich.edu

Abstract

A dynamic model for analysis of the performance of roller chain drive with a tensioners is presented. The model is based on the axially moving material model first given by Mote, but includes extensions that allow consideration of the effects of polygonal action, impact, and the periodic span length changes. Three equations of motion are obtained - one for the tensioner and one for each of the chain spans. The motion of the tensioner interacts with the motions of the chain spans through the chain tension, the contact angles, and the transverse displacement changes of the contact points. The effects of the periodic length change, tensioner stiffness, tensioner damping, tensioner position and external periodic load are investigated. Some of the results are compared to those obtained for a comparable chain drive without tensioner. Solutions are obtained by a finite difference method.

Nomenclature

c : chain span velocity

c_i : contact damping coefficient in impact

C_t : torsional damping coefficient of tensioner

I_2 : moment of inertia for driven sprocket system

I_t : effective moment of inertia of tensioner about its pivot point

k_i : contact stiffness coefficient in impact

K_t : torsional stiffness coefficient of tensioner

m_e : effective mass of tensioner

m_{eg} : effective mass of tensioner for gravity effect

m_i : effective mass in impact

m_l : mass per unit length of chain

M_{ts} : moment due to torsional spring

M_{td} : moment due to torsional damper

M_{ct} : moment due to chain tension

M_g : moment due to gravity

n_1, n_2 : driving and driven sprocket tooth numbers

r_1, r_2 : radius of driving and driven sprockets

r_t : radius of roller

P_c : chain tension

T_{ex} : magnitude of external periodic loading

T_p : tensioner preload torque

T_s : static tension

u, v : transverse displacements of chain span

V_{rel} : relative velocity of an engaging roller to sprocket surface

α_f: phase shift between engagement and disengagement

η : angle between relative velocity of roller and the sprocket surface

θ : tensioner arm angle

θ_0 : initial tensioner arm angle

ω_1 : angular velocity of driving sprocket

ω_2 : angular velocity of driven sprocket

ω_{ex} : frequency of external periodic loading

1. INTRODUCTION

Belt drives and chain drives are both commonly used methods of mechanical power transmission. Tensioners (or idlers) can be used on these two types of drives for several different reasons. In belt drives, tensioners are generally used to increase overall tension (to reduce slip). This has the additional benefit of increasing belt life. In roller chain drives, tensioners can improve drive performance by eliminating flop and sway on the slack side and reducing vibration and noise on the tight side [1-2]. In spite of the importance of the tensioner, there has not been much research reported in this area. Ulsoy, Whitesell and Hooven investigated a belt-tensioner system and reported mathieu type instabilities due to the belt tension variations caused by a periodic external load [3]. To date no theoretical investigations of chain drives with tensioners have been reported.

In this study the chain drive system comprises two chain spans and a torsional tensioner. The modeling of each chain span is based on an axially moving material [4]. The modeling of polygonal action and impact is more completely described in reference [5]. Periodic length change for each chain span is also considered. The interaction between the tensioner and the chain spans and the performance of the chain drive with a tensioner are examined and the results are reported.

2. TRANSVERSE VIBRATION IN ROLLER CHAIN DRIVE WITH A TENSIONER

The chain drive system with a tensioner includes the driving and driven sprockets, tensioner assembly, and chain spans (see figure 1). The tensioner assembly consists of a tensioner arm, a tensioner disk, a torsional spring, and a torsional damper. In order to simplify the analysis, a circular disk is adopted as the tensioner pulley and the contact line between the disk and the chain span is assumed to form a circular arc. The modeling of the tensioner and the chain span are done independently but they are coupled through the chain tension term, the inclination angles of the chain spans and the displacements of the contact points between the tensioner and the chain spans.

2.1 Dynamic Load

2.1.1 Speed Tensioning, Impact and External Periodic Load

The dynamic load due to speed tensioning is obtained in a way similar to the case of chain drive without a tensioner, i.e.,

$$D_s = \lambda m c^2 \tag{2-1}$$

The pulley support constant λ can be estimated as follows [6].

$$\lambda = k_b/(k_b + k_s + k_g) \tag{2-2}$$

where $k_b = (EA/L)(\cos\psi_1 + \cos\psi_2)^2$, $k_s = k_t/l_t^2$, $k_g = T_s(\zeta_1 + \zeta_1)$,

$\zeta_i = d(\cos\psi_i)/dx_s$, EA = chain strength, L = overall span length.

As for the impact, only the major impact between the engaging roller and the driving sprocket is considered. The dynamic load due to impact is determined in the same way as in the case of a chain drive without a tensioner [5] and it is given by

$$D_{imp} = \frac{V_{rel}\sin 2\eta}{2\omega_d} e^{-\zeta\omega_n t} \{ (k_i - c_i \zeta \omega_n) \sin \omega_d t + c_i \omega_d \cos \omega_d t \} \quad (0 < t < \frac{\pi}{\omega_d}) \tag{2-3-a}$$

$$D_{imp} = 0 \quad (\frac{\pi}{\omega_d} < t < \frac{\pi}{\omega_1 n_1}) \tag{2-3-b}$$

where $V_{rel} = \omega_1 p_c$, p_c : chain pitch, $\eta = 35 + 240/n1 + \varepsilon$ deg., $\varepsilon << 1$,

$\omega_n = (k_i/m_i)^{0.5}$, $\omega_d = \omega_n (1-\zeta^2)^{0.5}$, $\zeta = c_i/(2 (m_i k_i)^{0.5})$.

External dynamic loads are included by a single trigonometric term.

$$D_{ext} = T_{ex} \cos \omega_{ex} t \tag{2-4}$$

2.1.2 Polygonal Action

The major parameter related to polygonal action is the fractional pitch and it is determined by the positions of the tensioner and sprockets. The lengths of span #1 and #2 and the length of the arc formed around the tensioner disk are shown in figure 1. The fractional pitch is calculated based on the geometric information and there are two different general tensioner positions. One is the case where the tensioner pivot point stays on the right side of the vertical line passing through the center of the tensioner disk (tensioner position #1) and the other is the case where the pivot point resides on the left side of the vertical line (tensioner position #2).

$$f_p = \frac{L_1 + L_2 + (r_t + r_r)(\varepsilon_1 + \varepsilon_2) - i*\text{pitch}}{\text{pitch}} \qquad (2\text{-}5)$$

where i : any integer such that $0 \le f_p \le 1$,

$$\varepsilon_1 = \frac{\pi}{2} + \tan^{-1}\left(\frac{P_{1Y} - P_{4Y}}{P_{1X} - P_{4X}}\right) - \tan^{-1}\left(\frac{L_1}{r_1 + r_t + r_r}\right),$$

$$\varepsilon_2 = \frac{\pi}{2} + \tan^{-1}\left(\frac{P_{2Y} - P_{4Y}}{P_{4X} - P_{2X}}\right) - \tan^{-1}\left(\frac{L_2}{r_2 + r_t + r_r}\right),$$

$$L_1 = \sqrt{S_1^2 - (r_1 + r_t + r_r)^2}\,, \quad S_1 = \sqrt{(P_{1X} - P_{4X})^2 + (P_{1Y} - P_{4Y})^2}\,,$$

$$L_2 = \sqrt{S_2^2 - (r_2 + r_t + r_r)^2}\,, \quad S_2 = \sqrt{(P_{4X} - P_{2X})^2 + (P_{4Y} - P_{2Y})^2}\,,$$

$$P_{4X} = P_{3X} - l_t \cos\theta \text{ (for tps \#1) or } P_{3X} + l_t \cos\theta \text{ (for tps \#2)},$$

$$P_{4Y} = P_{3Y} - l_t \sin\theta\,.$$

The fractional pitch changes as time changes because ε_1 and ε_2 change. The fractional pitch was assumed to be constant in the case of a roller chain drive without a tensioner [5]. The phase angle (α_f) between engagement and disengagement is computed by multiplying one tooth angle of the driven sprocket by the fractional pitch.

The angular velocity relationship between the driving and driven sprockets is formulated by equating the chain velocities from the driving sprocket side and the driven sprocket side (figure 1). Using the x_1-y_1 coordinates and x_2-y_2 coordinates in the figure, the same equation used in the case of the chain drive without a tensioner is obtained. The

way to obtain the dynamic load due to the polygonal action for the rigid four bar model (applicable at low speeds) is the same as presented in reference [5] except that the constant fractional pitch is replaced with the time dependent fractional pitch given by equation (2-5). The angular motion of the driven sprocket and the dynamic load is given by

$$\theta_2 = \theta_{2int} \qquad (\theta_{2int} \le \frac{\pi}{2} + \frac{\pi}{n_2}) \tag{2-6-a}$$

$$\theta_2 = \theta_{2int} - \frac{2\pi}{n_2} \qquad (\theta_{2int} > \frac{\pi}{2} + \frac{\pi}{n_2}) \tag{2-6-b}$$

where $\theta_{2int} = \cos^{-1}\left\{\frac{r_1}{r_2}(\cos\theta_1 - \cos\theta_{10}) + \cos\theta_{20}\right\}$, $\theta_{10} = \theta_1(0) = \frac{\pi}{2} - \frac{\pi}{n_1}$,

$$\theta_{20} = \theta_2(0) = \frac{\pi}{2} - \frac{\pi}{n_2} + \alpha_f, \quad \alpha_f = \frac{2\pi}{n_2} f_p.$$

$$D_{pol} = \frac{I_2}{r_2}\alpha_2 = \frac{I_2}{r_2^2 \sin\theta_2}(r_1 \omega_1^2 \cos\theta_1 - r_2 \omega_2^2 \cos\theta_2) \tag{2-7}$$

where $\theta_1 = \omega_1 t + \frac{\pi}{2} - \frac{\pi}{n_1}$.

The way to obtain the dynamic load due to the polygonal action in case of the elastic four bar model (applicable at moderate and high speeds) is also the same as presented in reference [5] except that the time-dependent fractional pitch is used instead of the constant fractional pitch. The angular movement of the driven sprocket and the dynamic load are given by

$$\theta_2 = \int_0^t \dot{\theta}_2\, dt = \frac{\omega_1}{N^3 a_0^2}(q_0 t + q_1 \sin pt + q_2 \sin 2pt + q_3 \sin 3pt + q_4 \sin 4pt - p_0 t - p_1 \cos pt - p_2 \cos 2pt - p_3 \cos 3pt - p_4 \cos 4pt + c_{int}) \tag{2-8}$$

where $c_{int} = \frac{N^3 a_0^2}{\omega_1}(\alpha_f + \frac{\pi}{2} - \frac{\pi}{n_2}) + p_1 + p_2 + p_3 + p_4 - q_0 \tau\, dint(\frac{t}{\tau})$,

$$N = \frac{n_2}{n_1} = \frac{\frac{n_2 r_2}{\pi}\sin(\frac{\pi}{n_2})}{\frac{n_1 r_1}{\pi}\sin(\frac{\pi}{n_1})}, \quad p = n_1 \omega_1, \quad a_0 = \frac{n_1 r_1}{\pi}\sin\frac{\pi}{n_1},$$

dint(x) rounds the value of x to the nearest integer towards zero.

$$D_{pol} = k\,(x_2 - x_1 - L) = \frac{k\,\omega_1}{N\,p}\{(N\,a_1 - l_1)\sin pt + m_1 \cos pt + 0.5\,(N\,a_2 - l_2)\sin 2pt + 0.5\,m_2 \cos 2pt - m_1 - 0.5\,m_2\} \quad (2\text{-}9)$$

$$\text{where } a_1 = \frac{2\,a_0}{1 - n_1^2},\quad a_2 = \frac{2\,a_0}{1 - 4\,n_1^2}.$$

The coefficients l_i, m_i, p_i, q_i,are described in Appendix I.

2.2 Transverse Displacements of End Points and Periodic Length Change

There are four end points - two for span #1 and the other two for span #2. This set includes the contact point between span #1 and the driving sprocket (end point #1), the contact point between span #1 and the tensioner disk (end point #2), the contact point between span #2 and the tensioner disk (end point #3) and the contact point between span #2 and the driven sprocket (end point #4).

The vertical displacements of end point #1 and end point #4 are calculated as follows.

$$u_n = r_1\,(1 - \sin\theta_1) \quad (2\text{-}10)$$

$$v_0 = r_2\,(1 - \sin\theta_2) \quad (2\text{-}11)$$

The angle of end point #4 is given by equation (2-6) at low speeds and by equation (2-8) at medium and high speeds. The vertical displacements of end points #2 and #3 are determined by the motions of the contact points between the tensioner disk and the chain spans. The computation of the contact points is based upon two angles (θ_m and θ_n in figure 1) formed by the chain spans and sprocket geometries.

$$P_{5X} = P_{4X} + (r_t + r_r)\cos\theta_m,\quad P_{5Y} = P_{4Y} - (r_t + r_r)\sin\theta_m \quad (2\text{-}12)$$

$$P_{6X} = P_{4X} - (r_t + r_r)\cos\theta_n,\quad P_{6Y} = P_{4Y} - (r_t + r_r)\sin\theta_n \quad (2\text{-}13)$$

$$\text{where } \theta_m = \frac{\pi}{2} - \varepsilon_1,\ \theta_n = \frac{\pi}{2} - \varepsilon_2.$$

Suppose P_5 has moved from $[P_5]_i$ to $[P_5]_{i+1}$ and P_6 has moved from $[P_6]_i$ to $[P_6]_{i+1}$ during one time step.

$$\alpha_a = [P_{5X}]_{i+1} - [P_{5X}]_i , \quad \beta_a = [P_{5Y}]_{i+1} - [P_{5Y}]_i \tag{2-14}$$

$$\alpha_b = [P_{6X}]_{i+1} - [P_{6X}]_i , \quad \beta_b = [P_{6Y}]_{i+1} - [P_{6Y}]_i \tag{2-15}$$

There are four different cases for each form of tensioner position (tensioner position #1 or tensioner position #2) in the computation of vertical displacements in terms of α_a, α_b, β_a, and β_b. The related angles and the changes of vertical displacements are shown in figure 2 for tensioner position #1 and the expressions for the changes (d_5 and d_6) are described in Appendix II.

$$[u_0]_{i+1} = [u_0]_i + [d_5]_i \tag{2-16}$$

$$[v_n]_{i+1} = [v_n]_i + [d_6]_i \tag{2-17}$$

where i, i + 1 represents time $i*\Delta t$ and $(i+1)*\Delta t$ respectively.

The length changes occur for both span #1 and span #2 since all the end points are moving. In the case of the chain drive without tensioner, the span changes its length abruptly whenever there is engagement or disengagement between chain links and the sprockets. When the tensioner is present, each span changes its length, not only abruptly at the engagement and the disengagement of chain links, but also gradually at other times. The span lengths in a chain drive with a tensioner are determined by the end points.

$$\text{spl1 (length of span \#1)} = \sqrt{(z_{1x} - P_{5x})^2 + (z_{1y} - P_{5y})^2} \tag{2-18}$$

$$\text{spl2 (length of span \#2)} = \sqrt{(z_{2x} - P_{6x})^2 + (z_{2y} - P_{6y})^2} \tag{2-19}$$

where $z_{1x} = P_{1x} - r_1 \cos\theta_{z1}$, $z_{1y} = P_{1y} + r_1 \sin\theta_{z1}$,

$z_{2x} = P_{2x} + r_2 \cos\theta_{z2}$, $z_{2y} = P_{2y} + r_2 \sin\theta_{z2}$,

$\theta_{z1} \approx \theta_1 - \varepsilon_1$, $\theta_{z2} \approx \pi - \varepsilon_2 - \theta_2$.

2.3 Equations of Motion

The tensioner assembly is modeled as a single degree of freedom system with torsional damper and torsional spring. The tensioner rotates about its pivot and the equation of motion is formulated by considering the moment equilibrium about the pivot point.

$$I_t\ddot{\theta} = M_{ts} + M_{td} + M_{ct} + M_g \tag{2-20}$$

There are four moments related to the pivot point of the tensioner and they are due to the torsional spring, torsional damping, chain span tension (see figure 3) and gravity.

$$M_{ts} = K_t(\theta_0 - \theta) + T_p \tag{2-21}$$

$$M_{td} = -C_t\dot{\theta} \tag{2-22}$$

$$M_{bt} = P_c l_t\{\sin(\theta - \varepsilon_1) - \sin(\theta + \varepsilon_2)\} \text{ (tsp \#1) or}$$

$$P_c l_t\{\sin(\theta - \varepsilon_2) - \sin(\theta + \varepsilon_1)\} \text{ (tsp \#2)} \tag{2-23}$$

where P_c(chain tension) $= T_s + D_s + D_{pol} + D_{imp} + D_{ext}$.

$$M_g = m_{eg}\, g\, l_t \cos\theta$$

Substitution of the expressions for the moments into (2-20) leads to the final form of the equation of motion.

$$m_e l_t^2\ddot{\theta} + C_t\dot{\theta} + K_t\theta = K_t\theta_0 + P_t + P_c l_t\{\sin(\theta - \varepsilon_1) - \sin(\theta + \varepsilon_2)\} + m_{eg}\, g\, l_t\cos\theta \quad \text{for tensioner position \#1} \tag{2-24}$$

$$m_e l_t^2\ddot{\theta} + C_t\dot{\theta} + K_t\theta = K_t\theta_0 + P_t + P_c l_t\{\sin(\theta - \varepsilon_2) - \sin(\theta + \varepsilon_1)\} + m_{eg}\, g\, l_t\cos\theta \quad \text{for tensioner position \#2} \tag{2-25}$$

The motion of the tensioner was represented by one ordinary differential equation which is coupled with the equations of motion for the chain spans through the tension term

and inclination angles. Forward finite differencing was done about time to solve the equation.

There are two chain spans in a chain drive with a tensioner. The chain span in contact with driving sprocket is denoted as span#1 and the other is span#2. Because of the presence of the tensioner, sag can be neglected in both chain spans. The equation of motion for a chain drive without a tensioner can be used for each chain span. The transverse vibration of chain span #1 is represented by u and the transverse vibration of chain span #2 is represented by v.

$$\text{Span \#1 : } m_l u_{,tt} + 2 m_l c u_{,tx} + m_l c^2 u_{,xx} + c_d(u_{,t} + c u_{,x}) - (P + P_t) u_{,xx} = 0 \qquad (2\text{-}26)$$

$$\text{Span \#2 : } m_l v_{,tt} + 2 m_l c v_{,tx} + m_l c^2 v_{,xx} + c_d(v_{,t} + c v_{,x}) - (P + P_t) v_{,xx} = 0 \qquad (2\text{-}27)$$

$$\text{where } P = T_s + D_c,\ P_t = D_{pol} + D_{imp} + D_{ext}.$$

The boundary conditions for span #1 are given by the equations (2-10) and (2-16) and the boundary conditions for span #2 are given by the equations (2-11) and (2-17). The finite difference formulation followed the finite differencing scheme used in the reference [5].

3. COMPUTER SIMULATION

3.1 Time Step Control and Simulation Strategy

A nonuniform time step scheme was utilized to execute computation efficiently. The basic idea is to use smaller time steps near the instant of the impact between engaging roller and sprocket tooth and larger time steps away from that instant so that the effect of the impact is included while the total computation time is minimized without causing numerical instabilities. To achieve this objective, an exponential function was utilized.

The main objective of the simulation is to observe the change of the motions of the roller chain drive and the tensioner under different circumstances. In order to obtain the steady state response at an operating speed, the transient region during some amount of time from the beginning was ignored and the response after that was used to calculate the vibration amplitude. Next, the maximum amplitude from the equilibrium configuration of a chain span was chosen as a variable representing the vibration amplitude effectively over a wide range of operating speed. In order to represent the motion of the tensioner, two more

variables were introduced - the average angle of the tensioner arm in vibration and the angular vibration amplitude of the arm about the average angle.

3.2 Simulation Results and Discussion

The chain drive system used in this simulation consists of number 40 chain, two 24 tooth sprockets and a tensioner. The effect of the moment of inertia for a driven sprocket system is investigated for a chain drive with a tensioner and the results are shown in figure 4. First of all, the dual peaks corresponding to the short and long lengths for each chain span that were observed in [5] are no longer present. Instead, there is one peak corresponding to the average span length. This is because the span takes on the short span or long span length only instantaneously when a tensioner is present. The span length varies continuously between these two values during the remainder of the tooth period. The resonance of the tensioner is around 248 rpm and the angular vibration magnitude increases as the moment of inertia increases (especially around the resonances). This is because the increase in the moment of inertia induces an increase in the tension variation due to the polygonal action. The average angle of the tensioner decreases as the operating speed increases. This decrease is physically reasonable since the tension of the span increases as the speed increases due to speed tensioning and this tension increase pushes up the tensioner. The vibration amplitudes of span #1 and span #2 show similar trends. The vibration amplitude is not strongly affected by changes in the moment of inertia before the fourth resonance occurs, but the effect of changes in the moment of inertia is clear around the fourth resonance. In the case of the largest moment of inertia of figure 4 (solid line), even instability can even occur due to the parametric excitation.

The effects of tensioner stiffness are represented in figure 5. The location of the tensioner resonance increases as the stiffness increases and the amplitude at the resonance also increases as the stiffness increases since the excitation due to polygonal action increases as the speed increases. If the magnitude of the excitation remains the same at any speed, the amplitude will decrease as the stiffness increases. The amplitude of span #1 around the fourth resonance increases as the stiffness decreases while below the resonance the effect of the tensioner stiffness is insignificant. The amplitude of span #2 also shows the same trend. The effect of tensioner damping is shown in figure 6. Three cases (underdamped, critically damped, and overdamped) were considered. The effect of the damping is noticeable around the fourth resonance for span #1 and around the second and the fourth resonances for span #2.

The position of the tensioner pivot point was changed in the vertical direction and the effects are shown in figure 7. One of the most interesting subjects for research in the area

of roller chain drives is optimal tensioner position. Vertical changes in the location of the tensioner pivot point make a difference in the fractional pitch of the total chain span. Three cases were investigated. One is the system with 0.5258 initial fractional pitch (dotted line), another is the system with 0 initial fractional pitch (dashed line) and the other is the system with 0.6721 initial fractional pitch (dot-dashed) at 500 rpm. The initial fractional pitch is calculated at the equilibrium configuration for a given operating speed. As far as these three cases are concerned, the angular vibration amplitude is largest for the system with 0.5258 fractional pitch and smallest for the system with 0 fractional pitch. The effect on the vibration amplitude becomes large as the operating speed increases and there are some differences among the resonance positions because each span length changes as the vertical position of the tensioner pivot point changes.

The effect of the external periodic load on the case where the fractional pitch is 0 is also shown in figure 7. The effect is similar to that observed in the case of a roller chain drive without tensioner [5] and the addition of the external periodic load with the frequency $\omega_{ex} = \omega_1$ reduces the vibration amplitude around the resonances. The angular vibration amplitudes increase due to the external periodic load.

Figure 8 shows the effect of the two different general tensioner position forms, corresponding to tensioner position #1 (P_3 = (0.25, 0.1)) and tensioner position #2 (P_3 = (.1702, 0.1). The vibration amplitude with tensioner position #2 is larger than the amplitude with tensioner position #1 around the second resonance for span #1 and around the fourth resonance for span #1. It is interesting to notice that tensioner position #1 is preferred to tensioner position #2 in recent automotive serpentine belt designs.

The motions of the chain drive at medium operating speeds were also observed. Figure 9 shows the behavior of the chain drive when instabilities due to polygonal action in the elastic chain span occur. The system includes a relatively high inverse ratio of the tooth numbers (n_2/n_1 = 50/15) and small moment of inertia for the driven sprocket system (I2 = .0005 kg m^2). As shown in the figure, the range of the vibration amplitude affected by the second instability is wider than the range affected by the first instability since there is a transverse resonance just above the second instability and the effect of the resonance is combined with the second instability.

As the last simulation, a comparison between a chain drive with and without a tensioner was done for a system with the same center distance (30 pitches) between the driving and driven sprockets (figure 10). The tensioner position was set to let the initial fractional pitch at the operating speed of 500 rpm be zero. For the first and second cases (T_s = 25 N and T_s = 50 N) there are instabilities due to the combined effect of parametric (polygonal action) and external (curvature and transverse displacement changes at both ends)

excitations in a chain drive without tensioner, while there exist only relatively small vibrations in the chain drive with a tensioner. For the third and fourth cases (T_s = 100 N and T_s = 200 N), there are larger amplitudes at resonances but fewer number of resonances in the chain drive with a tensioner than in the chain drive without a tensioner since each chain span in the chain drive with a tensioner is smaller than the chain span in the chain drive without a tensioner.

4. SUMMARY AND CONCLUSION

A model for the chain drive with a tensioner was developed including some important features, such as polygonal action, impact, and periodic length length of each chain span. The tensioner interacts with the chain spans in several ways including chain tension. The periodic length change for each chain span does not produce two distinct peaks around each order resonance as was the case for systems without tensioners. Instead, there is one peak at each resonance, corresponding to the average span length. This is because the tensioner causes the span length to vary continuously between the shortest and longest span lengths during one tooth period, rather than to abruptly take on either one value or the other. At low operating speeds, higher tensioner stiffness could reduce the vibration amplitude especially around high order resonances, but the location of the tensioner resonance increases. The vibration at the resonance also increases because the tension variation increases as the operating speed increases. Changes in the vertical location of the tensioner pivot point can be used to change the fractional pitch of the total chain span. The vibration amplitude can be reduced and sometimes instability can also be prevented by adjusting the vertical position to let the time dependent fractional pitch be approximately zero. At medium operating speeds, there is a danger of instabilities due to polygonal action. The possibility is generally low, but it increases as the inverse ratio of the tooth numbers increases and as the moment of inertia for the driven sprocket decreases. Compared to chain drives without tensioners, the tensioner can not only prevent instabilities for low static tension operations but can also reduce the number of resonances.

5. ACKNOWLEDGEMENTS

The authors gratefully acknowledge the support of the National Science Foundation through Grants No. MSM-88-12957 and MSS-8996293. We also wish to thank N. C. Perkins for his thoughtful suggestions during the early stage of the model development.

BIBLIOGRAPHY

1. Les Gould, "Use an Idler to Solve Your Drive Problems", Modern Materials Handling, no. 45, Jun., 1990, p.75.
2. Kurt M. Marshek, "Standard Handbook of Machine Design - Chapter 32 Chain Drive", McGraw-Hill, 1986, pp.32.1 - 32.39.
3. A. G. Ulsoy, J. E. Whitesell, and M. D. Hooven, "Design of Belt-Tensioner Systems for Dynamic Stability", ASME Journal of Vibration, Stress, and Reliability in Design, vol.107, Jul. 1985, pp.282-290.
4. C. D. Mote, Jr., "Some Dynamic Characteristics of Band Saws," Forest Products Journal, January, 1965, pp 37 -41.
5. W. Choi and G. E. Johnson, "Vibration of Roller Chain Drives at Low, Medium and High Operating Speeds", Technical Report No. XXXXXXXXXX, Mechanical Engineering & Applied Mechanics Dept., University of Michigan, Ann Arbor, MI, 1992.
6. R. S. Beikman, N. C. Perkins and A. G. Ulsoy, "Equilibrium Analysis of Automotive Serpentine Belt Drive Systems Under Steady Operating Conditions", Proceedings of 22nd Midwestern Mechanics Conference, Oct. 1991, pp.533-534.

APPENDIX I

Coefficients in Equation (2-8) and (2-9)

The values of l_1, m_1, l_2, and m_2 are obtained from the following matrix equation.

$$X = (A^T A)^{-1} A^T F$$

where **X** is a 4×1 matrix whose elements are unknown variables (l_1, m_1, l_2,m_2).

The elements of the matrices in equation (A-1) are as follows.

$$a_{11} = \frac{c_1 k \omega_1}{2 N p}, \quad a_{12} = \frac{a_0 k \omega_1}{p} - \frac{b_1 k \omega_1}{2 N p}, \quad a_{13} = \frac{c_2 k \omega_1}{4 N p}, \quad a_{14} = \frac{a_0 k \omega_1}{2 p} - \frac{b_2 k \omega_1}{4 N p},$$

$$a_{21} = \frac{c_2 k \omega_1}{2 N p} - \frac{c_2 L_2 p \omega_1}{2 a_0^2 N^3}, \quad a_{22} = -\frac{a_0 k \omega_1}{p} + \frac{b_1 k \omega_1}{N p} - \frac{b_2 k \omega_1}{2 N p} + \frac{b_2 L_2 p \omega_1}{2 a_0^2 N^3} + \frac{I_2 p \omega_1}{a_0 N^2},$$

$$a_{23}=\frac{c_1 k \omega_1}{4 N p}+\frac{c_1 I_2 p \omega_1}{2 a_0^2 N^3},\quad a_{24}=\frac{b_1 k \omega_1}{4 N p}-\frac{b_1 I_2 p \omega_1}{2 a_0^2 N^3},\quad a_{31}=-\frac{c_1 k \omega_1}{2 N p}-\frac{c_1 I_2 p \omega_1}{a_0^2 N^3},$$

$$a_{31}=-\frac{c_1 k \omega_1}{2 N p}-\frac{c_1 I_2 p \omega_1}{a_0^2 N^3},\quad a_{32}=-\frac{b_1 k \omega_1}{2 N p}+\frac{b_2 k \omega_1}{N p}-\frac{b_1 I_2 p \omega_1}{a_0^2 N^3},$$

$$a_{32}=-\frac{b_1 k \omega_1}{2 N p}+\frac{b_2 k \omega_1}{N p}-\frac{b_1 I_2 p \omega_1}{a_0^2 N^3},\quad a_{33}=0,\quad a_{34}=-\frac{a_0 k \omega_1}{2 p}+\frac{b_2 k \omega_1}{2 N p}+\frac{2 I_2 p \omega_1}{a_0 N^2},$$

$$a_{41}=-\frac{c_2 k \omega_1}{2 N p}-\frac{3 c_2 I_2 p \omega_1}{2 a_0^2 N^3},\quad a_{42}=-\frac{b_2 k \omega_1}{2 N p}-\frac{3 b_2 I_2 p \omega_1}{a_0^2 N^3},\quad a_{43}=-\frac{c_1 k \omega_1}{4 N p}-\frac{3 c_1 I_2 p \omega_1}{2 a_0^2 N^3},$$

$$a_{43}=-\frac{c_1 k \omega_1}{4 N p}-\frac{3 c_1 I_2 p \omega_1}{2 a_0^2 N^3},\quad a_{44}=-\frac{b_1 k \omega_1}{4 N p}-\frac{3 b_1 I_2 p \omega_1}{2 a_0^2 N^3},\quad a_{51}=a_{52}=0,$$

$$a_{53}=-\frac{c_2 k \omega_1}{4 N p}-\frac{2 c_2 I_2 p \omega_1}{a_0^2 N^3},\quad a_{54}=-\frac{b_2 k \omega_1}{4 N p}-\frac{2 b_2 I_2 p \omega_1}{a_0^2 N^3},$$

$$a_{61}=\frac{a_0 k \omega_1}{p}-\frac{b_2 k \omega_1}{2 N p}+\frac{b_2 I_2 p \omega_1}{2 a_0^2 N^3}-\frac{I_2 p \omega_1}{a_0 N^2},\quad a_{62}=\frac{c_1 k \omega_1}{N p}-\frac{c_2 k \omega_1}{2 N p}+\frac{c_2 I_2 p \omega_1}{2 a_0^2 N^3},$$

$$a_{63}=\frac{b_1 k \omega_1}{4 N p}+\frac{b_1 I_2 p \omega_1}{2 a_0^2 N^3},\quad a_{64}=\frac{3 c_1 k \omega_1}{4 N p}+\frac{c_1 I_2 p \omega_1}{2 a_0^2 N^3},\quad a_{71}=\frac{b_1 k \omega_1}{2 N p}+\frac{b_1 I_2 p \omega_1}{a_0^2 N^3},$$

$$a_{72}=-\frac{c_1 k \omega_1}{2 N p}+\frac{c_2 k \omega_1}{N p}-\frac{c_1 I_2 p \omega_1}{a_0^2 N^3},\quad a_{73}=\frac{a_0 k \omega_1}{2 p}-\frac{2 I_2 p \omega_1}{a_0 N^2},\quad a_{74}=\frac{c_2 k \omega_1}{2 N p},$$

$$a_{81}=\frac{b_2 k \omega_1}{2 N p}+\frac{3 b_2 I_2 p \omega_1}{2 a_0^2 N^3},\quad a_{82}=-\frac{c_2 k \omega_1}{2 N p}-\frac{3 c_2 I_2 p \omega_1}{2 a_0^2 N^3},\quad a_{83}=\frac{b_1 k \omega_1}{4 N p}+\frac{3 b_1 I_2 p \omega_1}{2 a_0^2 N^3},$$

$$a_{84}=-\frac{c_1 k \omega_1}{4 N p}-\frac{3 c_1 I_2 p \omega_1}{2 a_0^2 N^3},\quad a_{91}=a_{92}=0,\quad a_{93}=\frac{b_2 k \omega_1}{4 N p}+\frac{2 b_2 I_2 p \omega_1}{a_0^2 N^3},$$

$$a_{94}=-\frac{c_2 k \omega_1}{4 N p}-\frac{2 c_2 I_2 p \omega_1}{a_0^2 N^3},\quad x_1=l_1,\quad x_2=m_1,\quad x_3=l_2,\quad x_4=m_2,$$

$$f_1=\frac{a_1 c_1 k \omega_1}{2 p}+\frac{a_2 c_2 k \omega_1}{4 p},\quad f_2=\frac{a_2 c_1 k \omega_1}{4 p}+\frac{a_1 c_2 k \omega_1}{2 p}+\frac{c_1 I_2 p \omega_1}{a_0 N^2},$$

$$f_3 = -\frac{a_1 c_1 k \omega_1}{2p} + \frac{2 c_2 I_2 p \omega_1}{a_0 N^2},\quad f_4 = -\frac{a_2 c_1 k \omega_1}{4p} - \frac{a_1 c_2 k \omega_1}{2p},\quad f_5 = -\frac{a_2 c_2 k \omega_1}{4p},$$

$$f_6 = \frac{a_2 b_1 k \omega_1}{4p} - \frac{a_1 b_2 k \omega_1}{2p} + \frac{a_0 a_1 k N \omega_1}{p} - \frac{b_1 I_2 p \omega_1}{a_0 N^2},\quad f_8 = \frac{a_2 b_1 k \omega_1}{4p} + \frac{a_1 b_2 k \omega_1}{2p},$$

$$f_7 = \frac{a_1 b_1 k \omega_1}{2p} + \frac{a_0 a_2 k N \omega_1}{2p} - \frac{2 b_2 I_2 p \omega_1}{a_0 N^2},\quad f_9 = \frac{a_2 b_2 k \omega_1}{4p}.$$

The values of p_i and q_i are represented as follows.

$$q0 = -0.5\,(b_1 l_1 + b_2 l_2 + c_1 m_1 + c_2 m_2) + (a_0 N)^2$$

$$q1 = \frac{1}{p}\{-0.5\,(b_2 l_1 + b_1 l_2 + c_2 m_1 + c_1 m_2) - a_0 n\,(b_1 - l_1)\}$$

$$q2 = \frac{1}{2p}\{-0.5\,(b_1 l_1 - c_1 m_1) - a_0 N\,(b_2 - l_2)\},$$

$$q3 = \frac{1}{3p}\{-0.5\,(b_2 l_1 + b_1 l_2 - c_2 m_1 - c_1 m_2)\},\quad q4 = \frac{1}{4p}\{-0.5\,(b_2 l_2 - c_2 m_2)\}$$

$$p1 = \frac{1}{p}\{-0.5\,(c_2 l_1 - c_1 l_2 - b_2 m_1 + b_1 m_2) - a_0 N\,(c_1 - m_1)\}$$

$$p_2 = \frac{1}{2p}\{-0.5\,(c_1 l_1 + b_1 m_1) - a_0 N\,(c_2 - m_2)\}$$

$$p_3 = \frac{1}{3p}\{-0.5\,(c_2 l_1 + c_1 l_2 + b_2 m_1 + b_1 m_2)\},\quad p4 = \frac{1}{4p}\{-0.5\,(c_2 l_2 + b_2 m_2)\}$$

APPENDIX II

Computation of Vertical Displacements of Contact Points Between Tensioner Disk and Chain Spans

There are four different cases to be considered in the computation of vertical displacements for each tensioner position (tensioner position #1 or tensioner position #2). For tensioner position #1, the related angles and the changes of vertical displacements are shown in figure 7 and computed as follows

Case 1 ($P_{3x} > P_{5x}$): $\gamma_a = \frac{\pi}{2} - \theta_m + \tan^{-1}\left(-\frac{\beta_a}{\alpha_a}\right) \rightarrow$

$$d_5 = \sqrt{\alpha_a^2 + \beta_a^2}\,\sin\gamma_a\ (\alpha_a > 0)\ \text{ or }\ -\sqrt{\alpha_a^2 + \beta_a^2}\,\sin\gamma_a\ (\alpha_a < 0)$$

Case 2 ($P_{3x} < P_{5x}$): $\gamma_a = \frac{\pi}{2} - \theta_m - \tan^{-1}\left(\frac{\beta_a}{\alpha_a}\right) \rightarrow$

$$d_5 = \sqrt{\alpha_a^2 + \beta_a^2}\,\sin\gamma_a\ (\alpha_a > 0)\ \text{ or }\ -\sqrt{\alpha_a^2 + \beta_a^2}\,\sin\gamma_a\ (\alpha_a < 0)$$

Case 3 ($\theta_n > \theta$): $\gamma_b = -\frac{\pi}{2} + \theta_n + \tan^{-1}\left(-\frac{\beta_b}{\alpha_b}\right) \rightarrow$

$$d_6 = \sqrt{\alpha_b^2 + \beta_b^2}\,\sin\gamma_b\ (\alpha_b > 0)\ \text{ or }\ -\sqrt{\alpha_b^2 + \beta_b^2}\,\sin\gamma_b\ (\alpha_b < 0)$$

Case 4 ($\theta_n < \theta$): $\gamma_b = \frac{\pi}{2} - \theta_n - \tan^{-1}\left(-\frac{\beta_b}{\alpha_b}\right) \rightarrow$

$$d_6 = -\sqrt{\alpha_b^2 + \beta_b^2}\,\sin\gamma_b\ (\alpha_b > 0)\ \text{ or }\ \sqrt{\alpha_b^2 + \beta_b^2}\,\sin\gamma_b\ (\alpha_b < 0)$$

In case 1 and case 2 the same expressions are derived but in case 3 and case 4 different expressions are presented. Finally the next vertical positions of end points #2 and #3 are obtained by adding the displacement changes calculated above to the present positions.

For tensioner position #2, the procedure to determine d_5 and d_6 is exactly the same as for the tensioner position #1.

Case 1 ($P_{3x} > P_{6x}$): $\gamma_b = \frac{\pi}{2} - \theta_n - \tan^{-1}\left(-\frac{\beta_b}{\alpha_b}\right) \rightarrow$

$$d_6 = -\sqrt{\alpha_b^2 + \beta_b^2}\,\sin\gamma_b\ (\alpha_b > 0)\ \text{ or }\ \sqrt{\alpha_b^2 + \beta_b^2}\,\sin\gamma_b\ (\alpha_b < 0)$$

Case 2 ($P_{3x} < P_{6x}$): $\gamma_b = \frac{\pi}{2} - \theta_n + \tan^{-1}\left(\frac{\beta_b}{\alpha_b}\right) \rightarrow$

$$d_6 = -\sqrt{\alpha_b^2 + \beta_b^2}\,\sin\gamma_b\ (\alpha_b > 0)\ \text{ or }\ \sqrt{\alpha_b^2 + \beta_b^2}\,\sin\gamma_b\ (\alpha_b < 0)$$

Case 3 ($\theta_m > \theta$): $\gamma_a = -\frac{\pi}{2} + \theta_m - \tan^{-1}\left(\frac{\beta_a}{\alpha_a}\right) \rightarrow$

$$d_5 = -\sqrt{\alpha_a^2 + \beta_a^2}\,\sin\gamma_a\ (\alpha_a > 0)\ \text{ or }\ \sqrt{\alpha_a^2 + \beta_a^2}\,\sin\gamma_a\ (\alpha_a < 0)$$

Case 4 ($\theta_m < \theta$) : $\gamma_a = \frac{\pi}{2} - \theta_m - \tan^{-1}\left(\frac{\beta_a}{\alpha_a}\right) \rightarrow$

$$d_5 = \sqrt{\alpha_a^2 + \beta_a^2}\,\sin\gamma_a\ (\alpha_a > 0)\ \text{ or }\ -\sqrt{\alpha_a^2 + \beta_a^2}\,\sin\gamma_a\ (\alpha_a < 0)$$

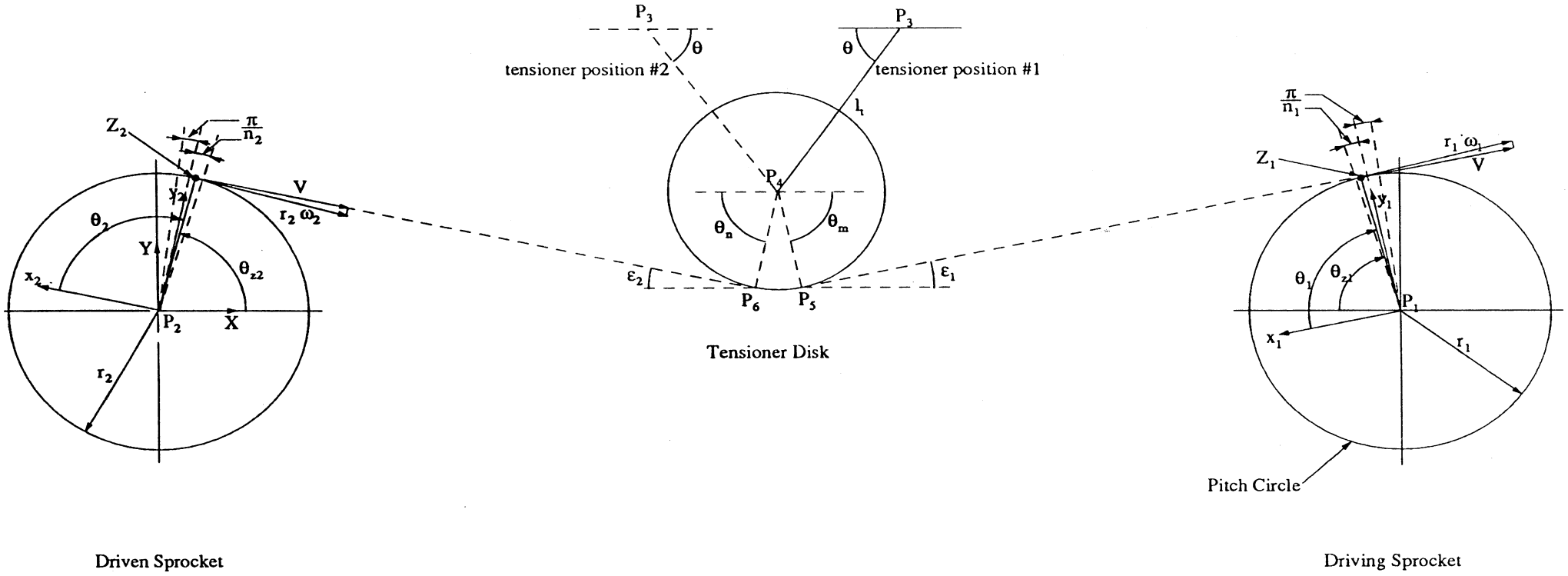

Figure 1 Configuration of Chain Drive with a Tensioner

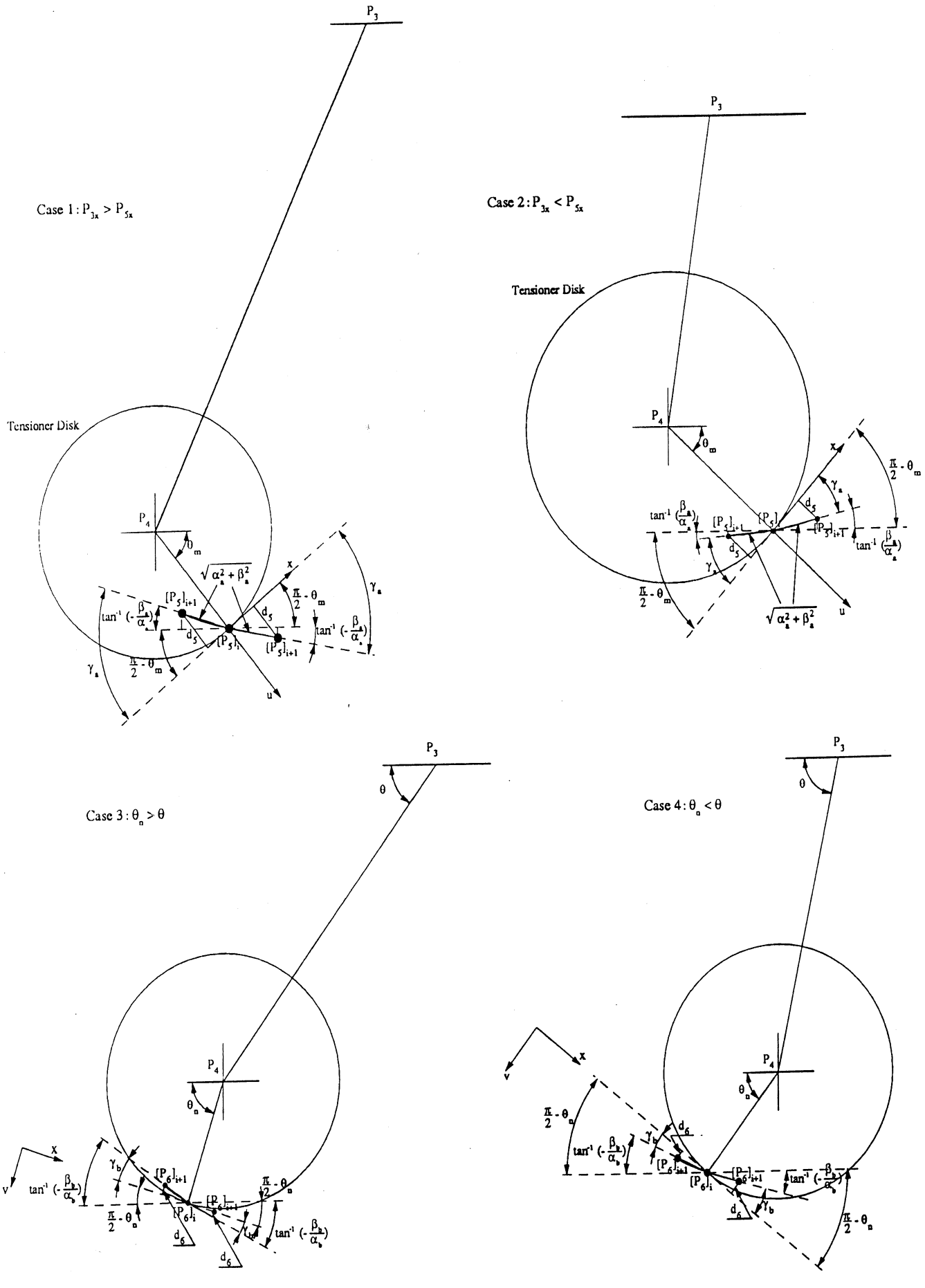

Figure 2 Angles Related with Contact Points Between Chain Span and Tensioner

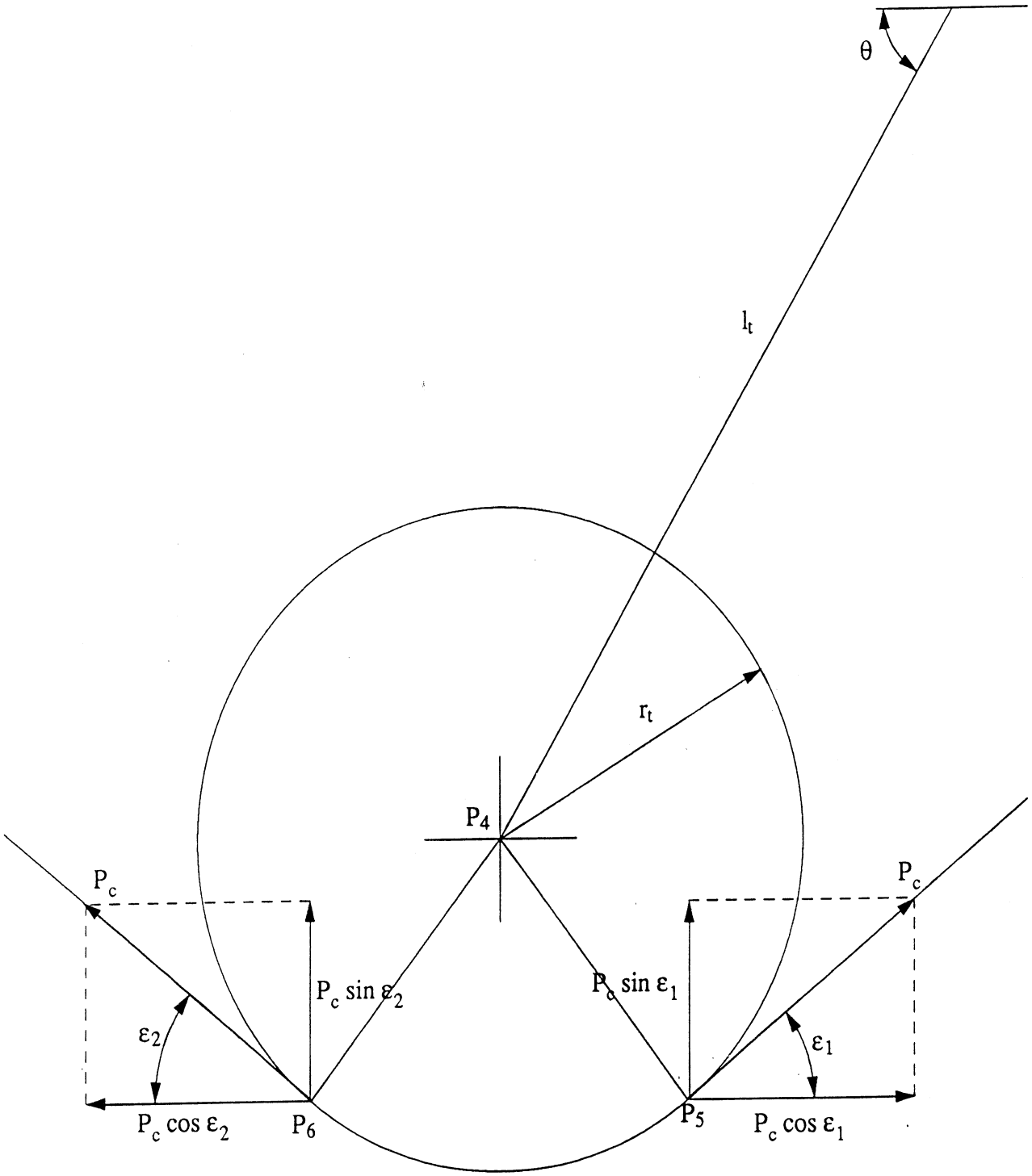

Figure 3 Calculation of Moment Applied to a Tensioner by Chain Tension

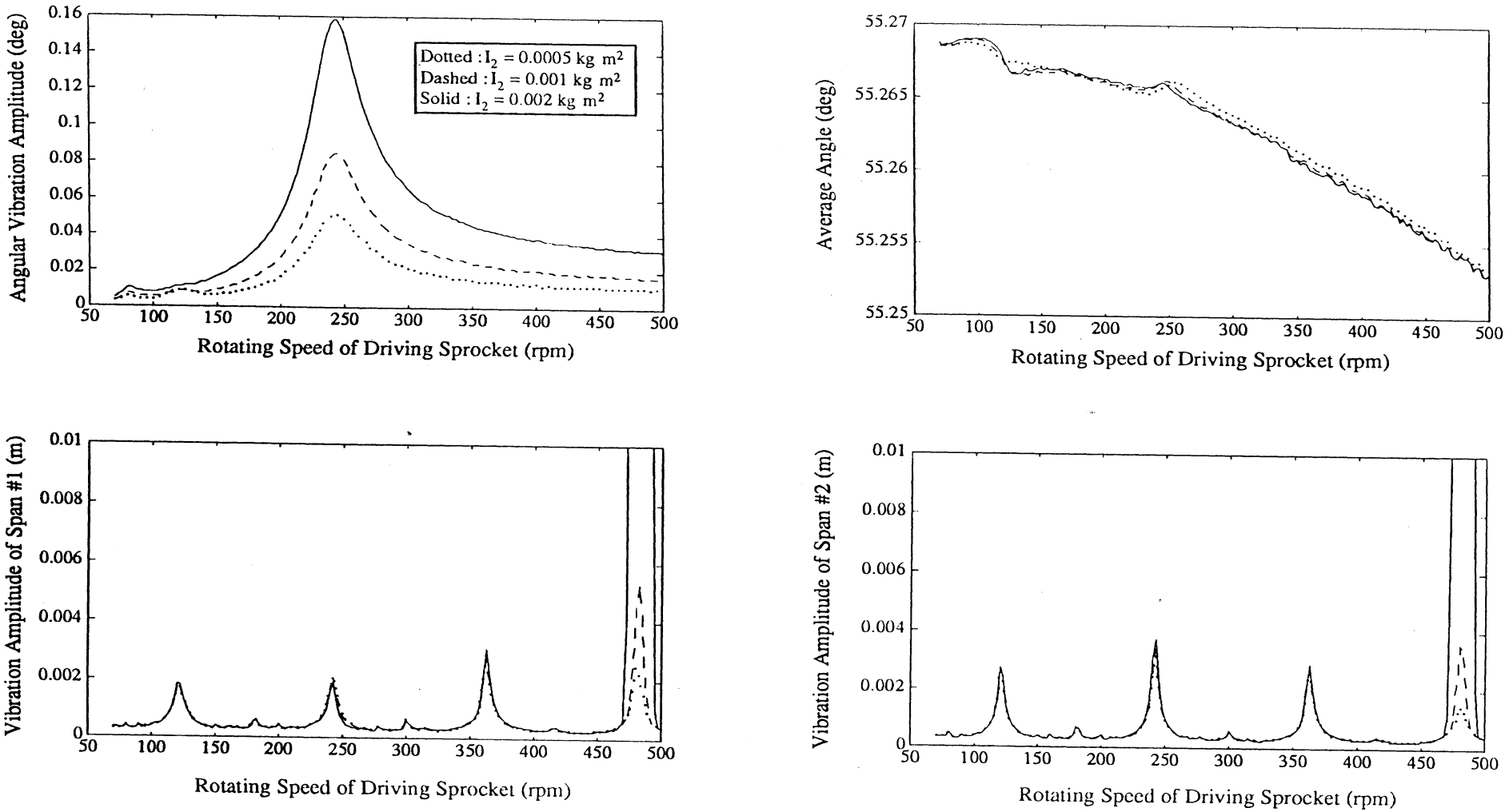

Figure 4 Effect of Moment of Inertia for Driven Sprocket System

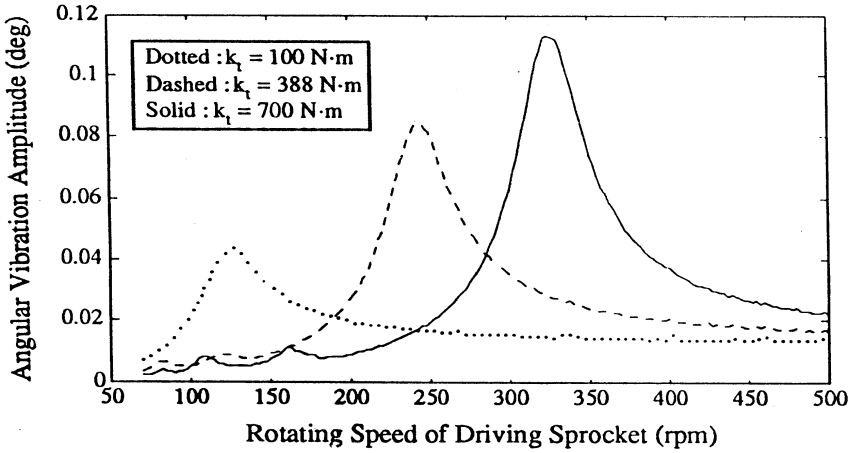

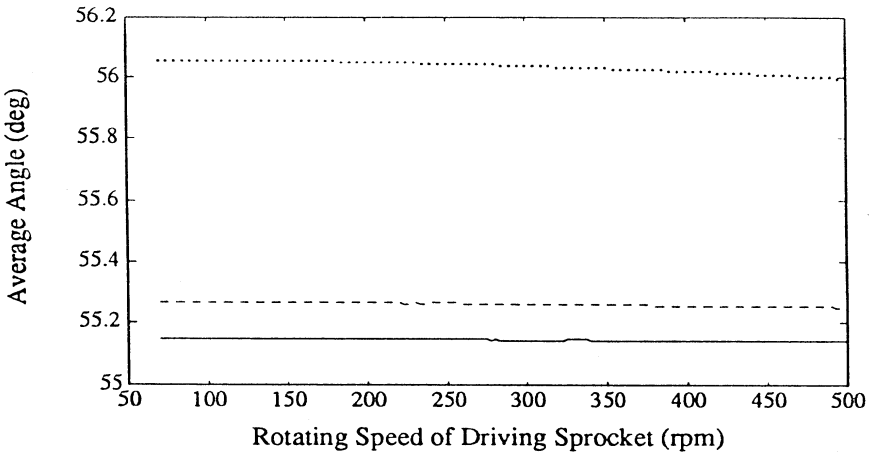

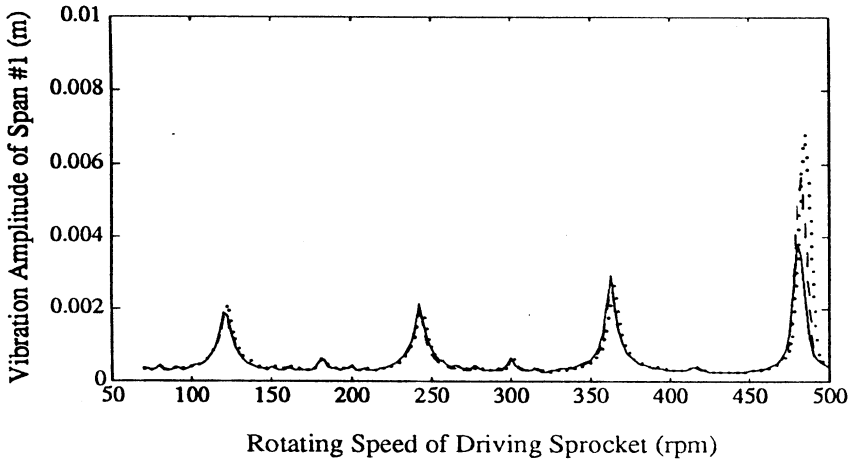

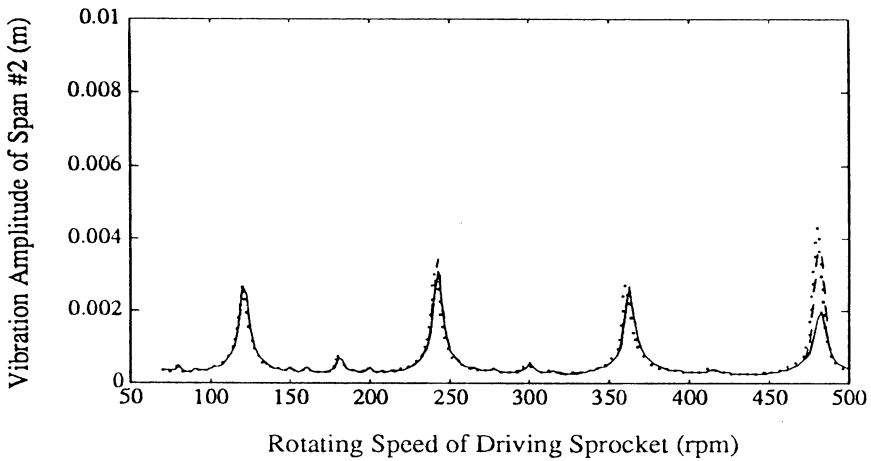

Figure 5 Effect of Tensioner Stiffness

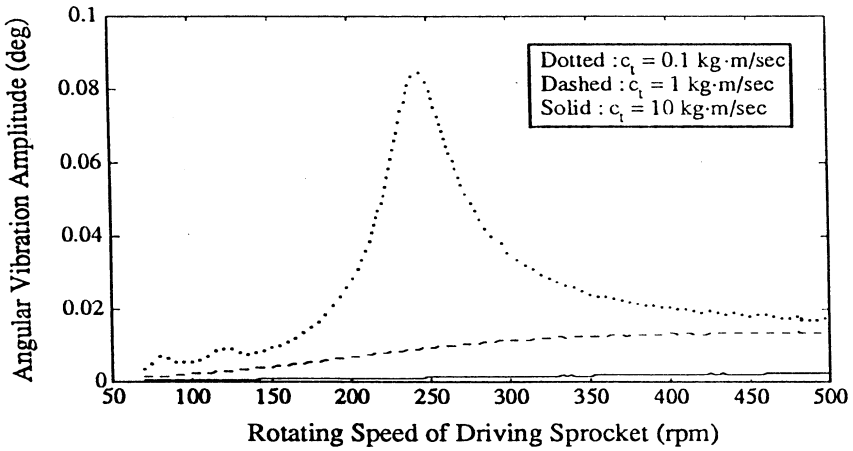

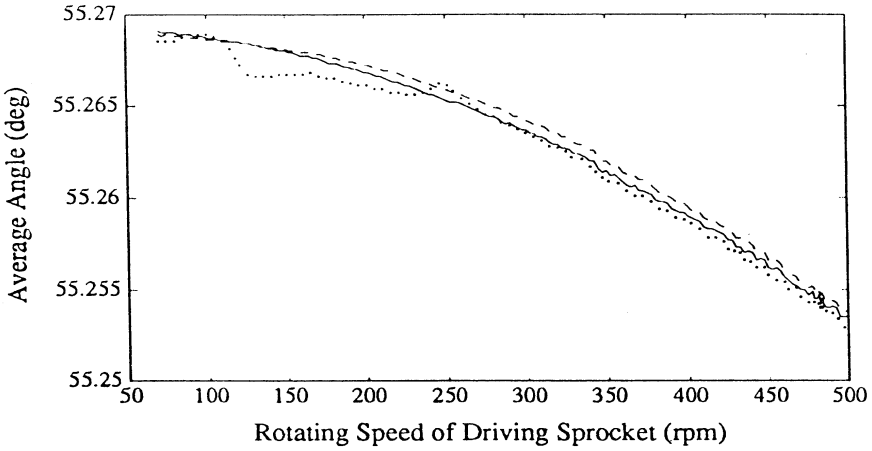

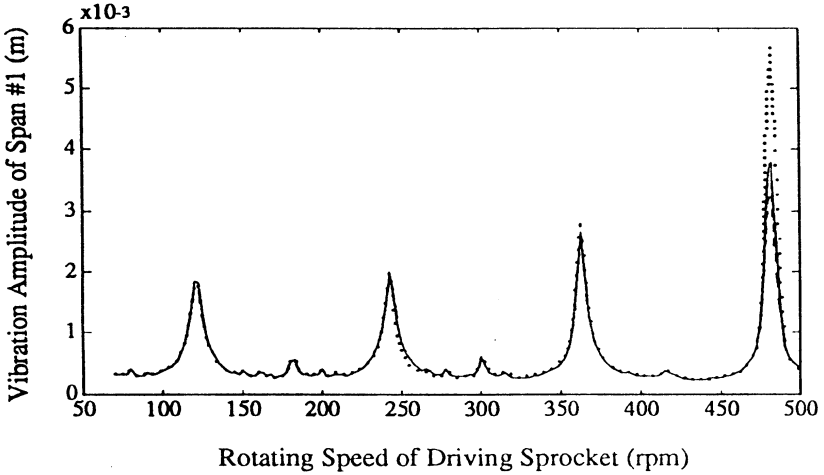

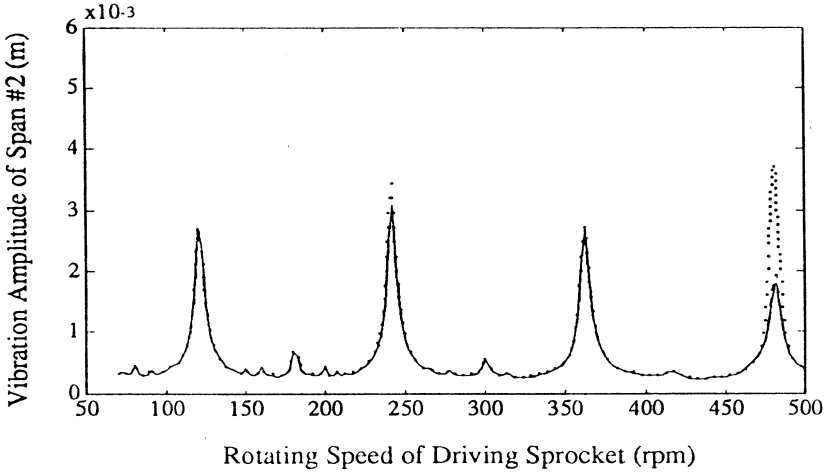

Figure 6 Effect of Tensioner Damping

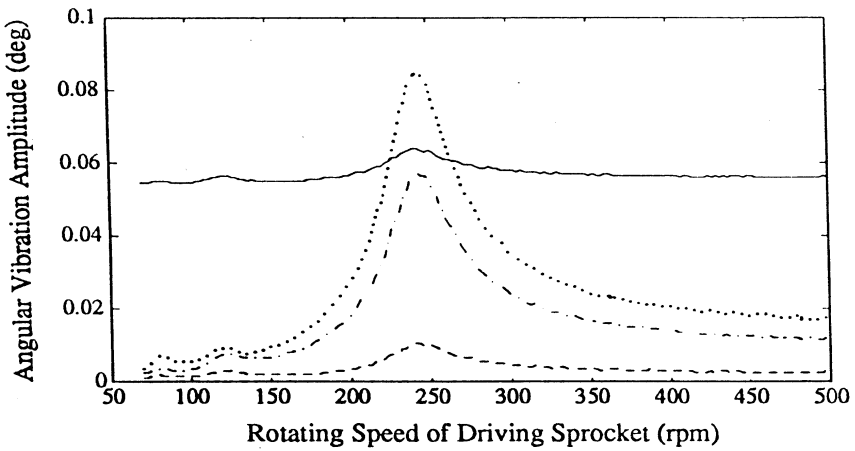

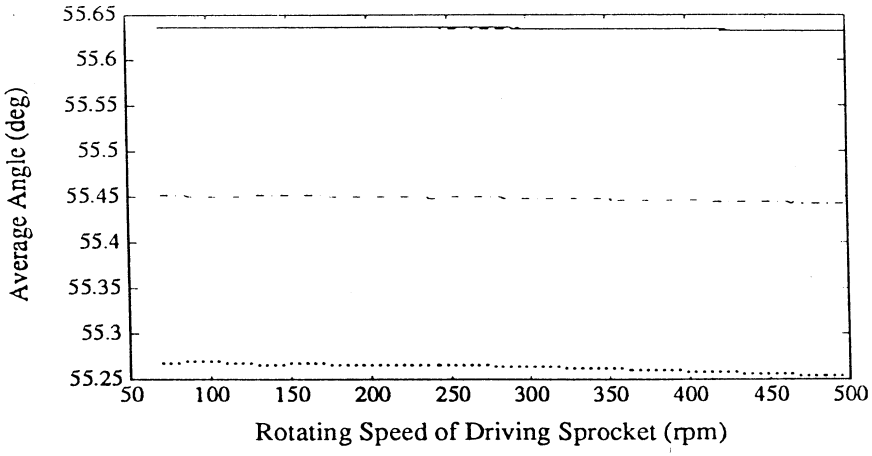

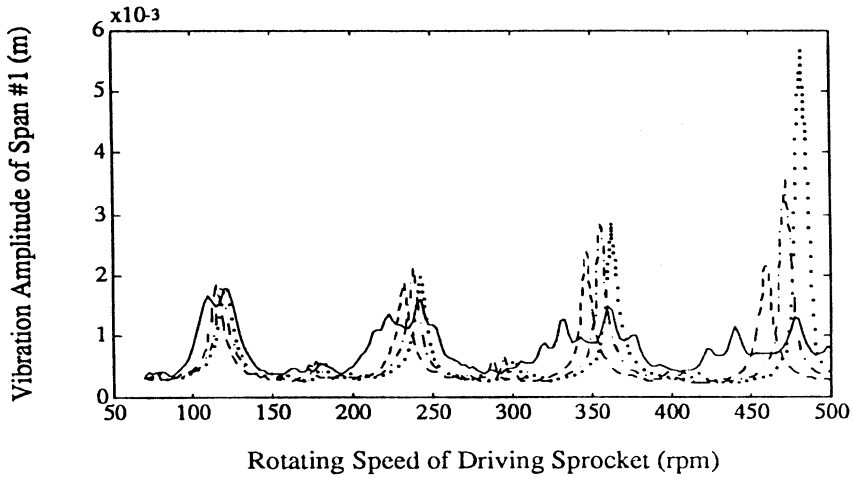

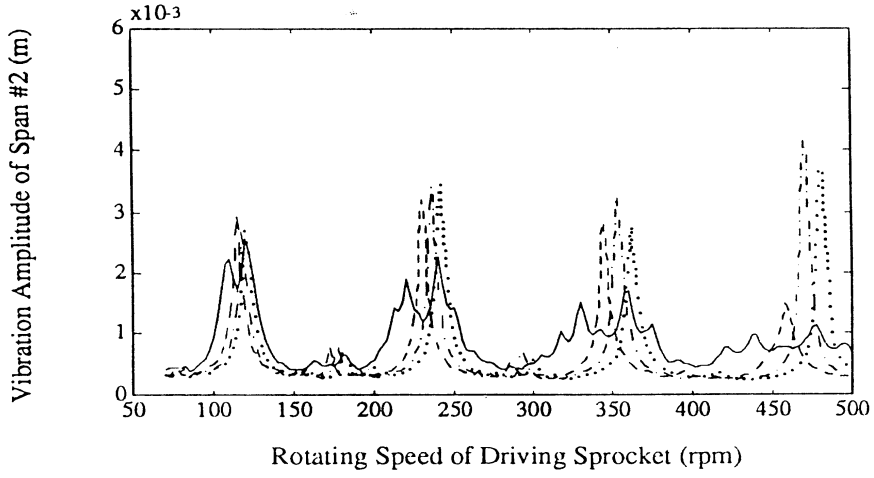

Figure 7 Effect of Tensioner Position and External Load

Dotted : $P_{3Y} = 0.1$ ($f_p = 0.5258$ at $\omega_1 = 500$ rpm)
Dot-Dashed : $P_{3Y} = 0.115$ ($f_p = 0.6721$ at $\omega_1 = 500$ rpm)
Dashed : $P_{3Y} = 0.1303$ ($f_p = 0$ at $\omega_1 = 500$ rpm)
Solid : $P_{3Y} = 0.1303$ w/ ext. load

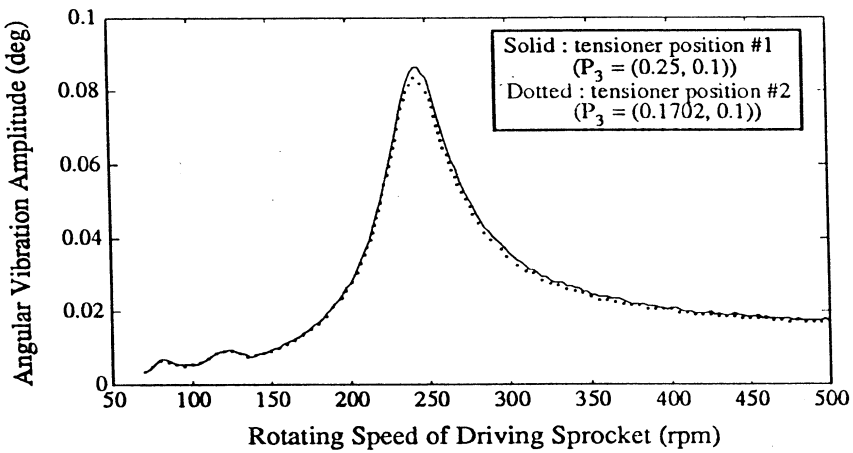

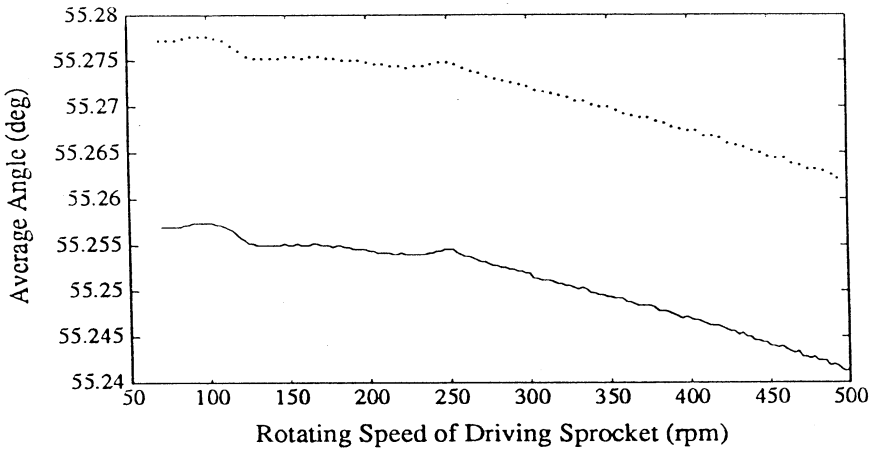

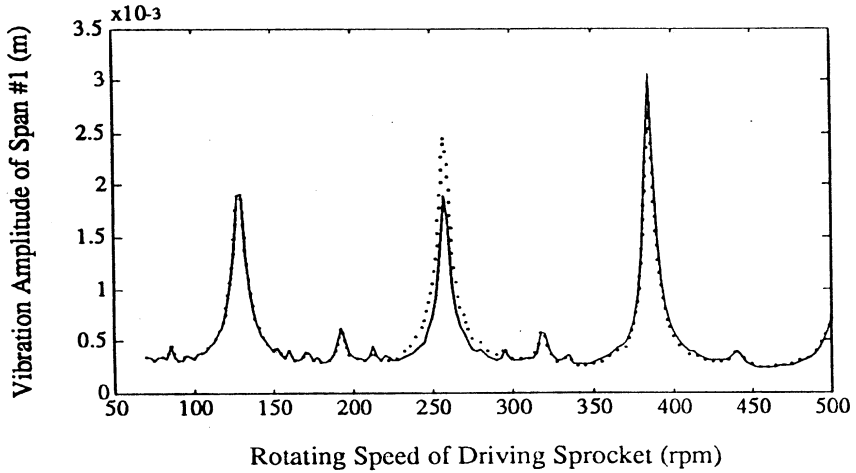

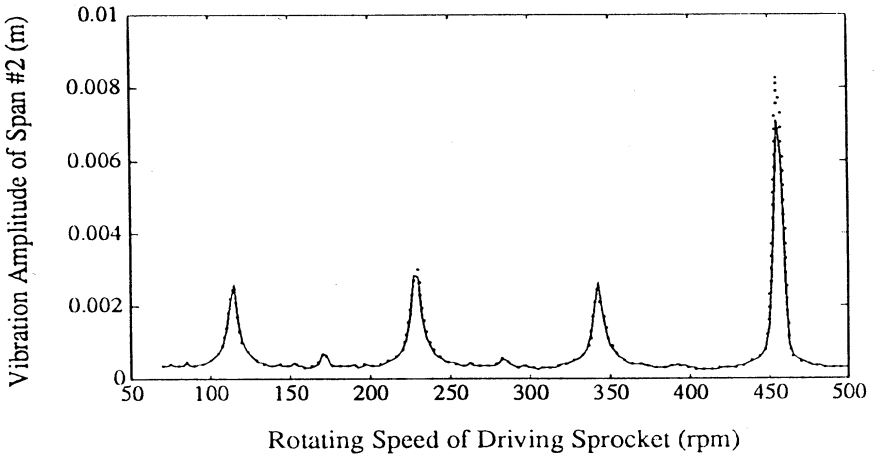

Figure 8 Effect of Different Tensioner Positions

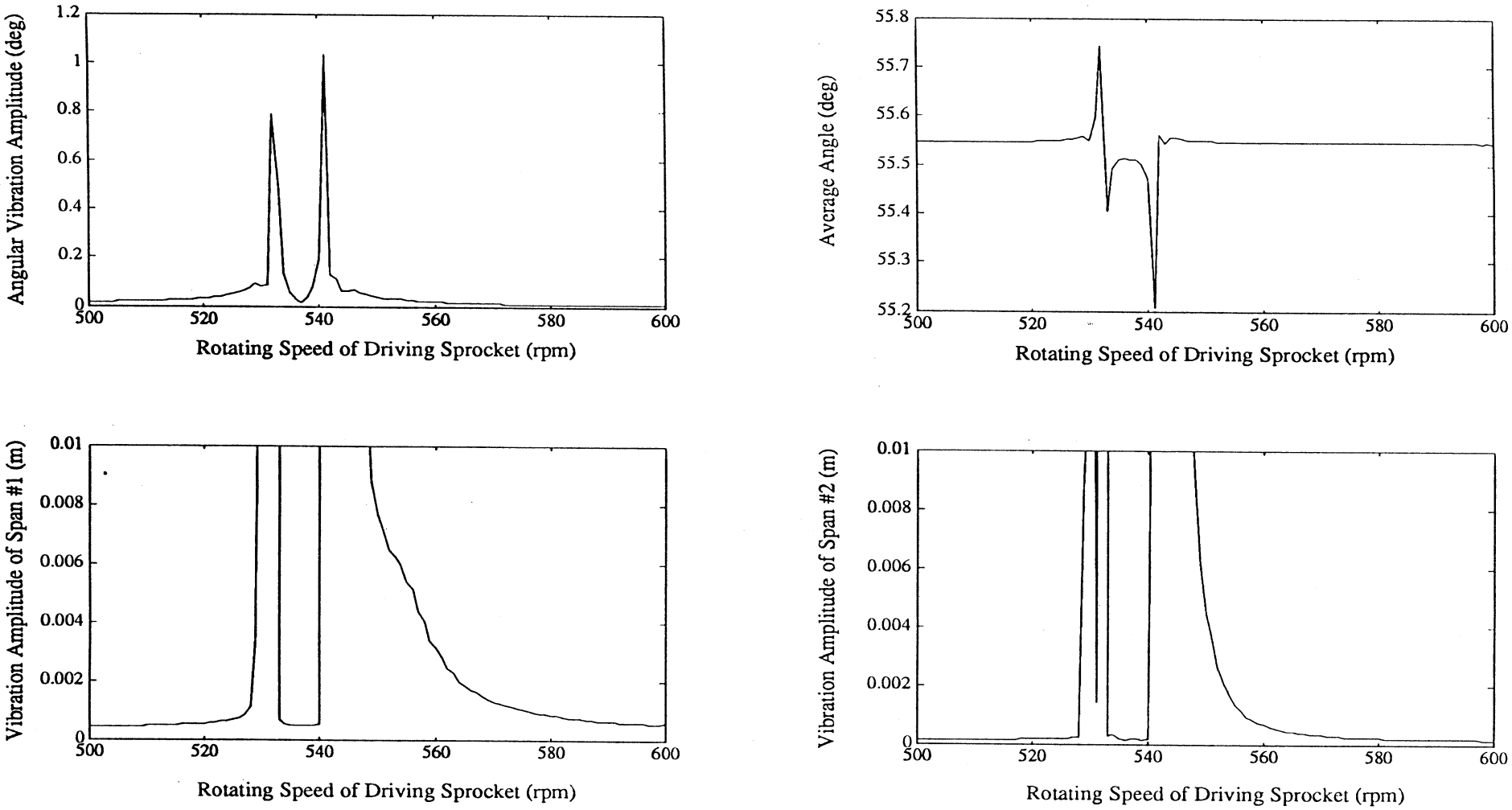

Figure 9 Behavior of Chain Drive with a Tensioner at Medium Operating Speeds
($n_2/n_1 = 50/15$, $I_2 = 0.0005$ kg·m²)

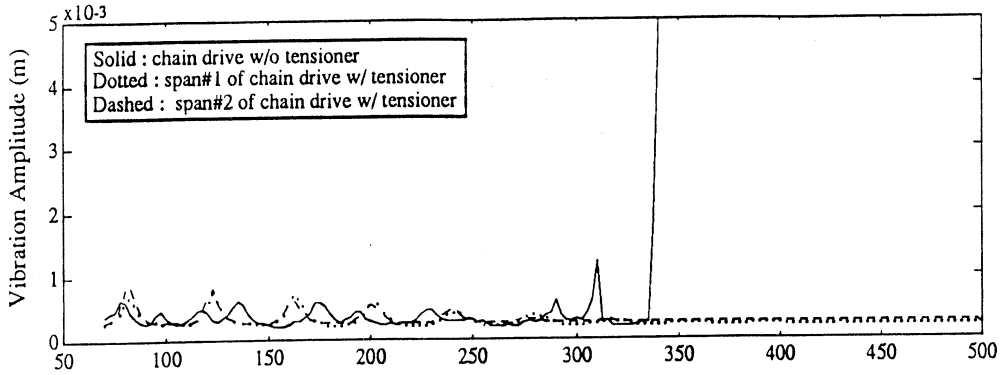

(a) T_s = 25 N

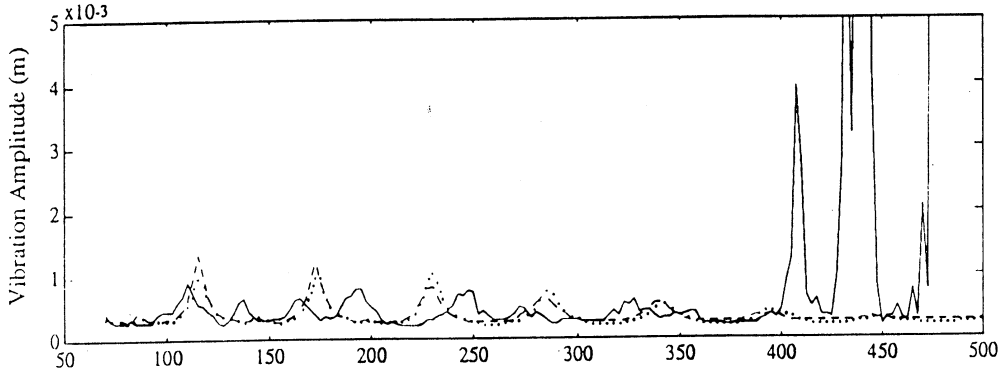

(b) T_s = 50 N

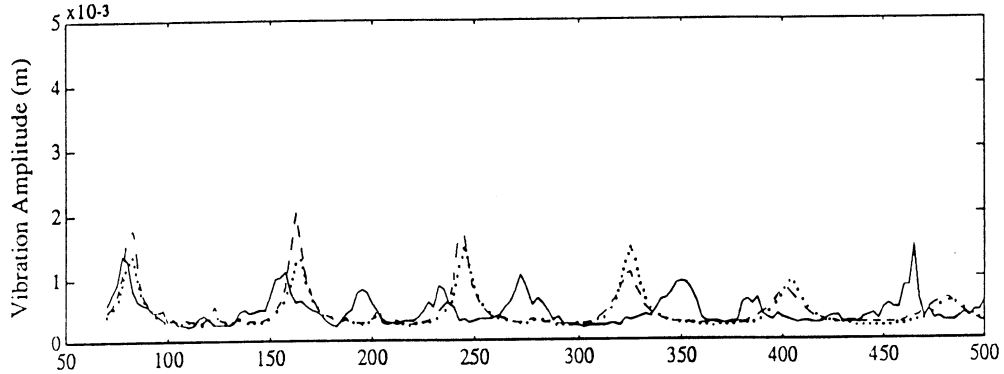

(c) T_s = 100 N

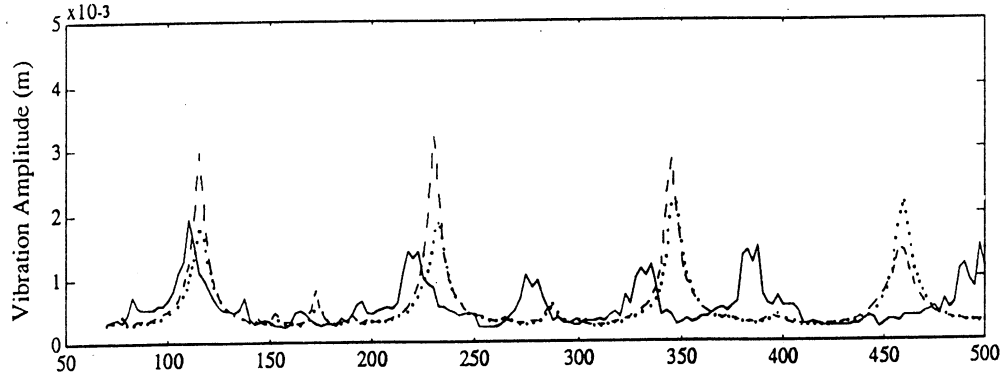

(d) T_s = 200 N

Figure 10 Comparison between Chain Drives with and without a Tensioner